

Polarization for TRINAT

Fall 2023 TRIUMF Work Term Report

Hannah Gallop

August 21st 2023

Table of Contents

1	Quarto Control	1
1.1	Magnetic Field	1
1.1.1	The Setup	1
1.1.2	The Results	2
1.2	Trap EOM Control	2
2	Fiber-coupled EOM at High Temperatures	3
2.1	Photorefraction Background	3
2.2	Heating the EOM	4
2.3	Possible Project	4
3	Polarization	4
3.1	Extracting Data	4
3.2	Different Cuts	5
3.2.1	Looking at Position	5
3.2.2	Push Beam	6
3.2.3	Photoion Events	6
3.3	The odd Run 4389	6
3.4	Best Estimate of Polarization	8
3.4.1	Differences on how normalize the count rate	9
3.5	Estimation of Background	10
3.5.1	Why don't we see a peak at the start of the optical pumping time	11
4	Detectors	11
4.0.1	Summary of Scintillation Crystals	11
4.1	Sodium Iodide dope with Thallium (NaI:Tl) Scintillation Crystal	11
4.1.1	Assembly of NaI	11
4.1.2	Calibration of NaI	12
4.2	Bismuth Germanate (BGO) Crystal	13
4.2.1	Calibration of BGO	14
5	Pumping Schemes for 40K vs 47K	15
5.1	Locking 47K	15
5.2	Locking 40K	16
5.3	Adjusting EOM circuit between 40K and 47K	16
6	Camera/ Octave Scripts	17
6.1	Accessing and executing the scripts	17
6.2	47K Run	18

1 Quarto Control

1.1 Magnetic Field

Problem: Melissa Anholm was seeing evidence of long-term eddy currents induced in the chamber by the magnetic coils [1]. The quadrupole magnetic field of the trap and the uniform optical pumping field are generated with Antihelmholtz coils. We have been using the Quarto to control the input current signal for each coil. Felix Klose researched and got the Quarto started, and the code we are currently using are edited versions of his code. The code we are currently using as of August 2023 is labelled 'BField_final.ino' and can be found under the Arduino folder on trcomp, and my laptop.

0-2500 [us]	Trap Magnetic field 'positive'
2501-3000 [us]	Delay between trap field and optical pumping field
3001-4000 [us]	Optical Pumping time
4001-6500 [us]	Trap Magnetic field 'negative'
6501-7000 [us]	Delay between trap field and optical pumping field
7001-8000 [us]	Optical Pumping time

Table 1: Timing For B-Field Control

The goal was to flip the magnetic trapping field every second time to reduce the long term eddy currents. Optical pumping signal needs to stay the same during each cycle. Since we need the magnetic field to go to zero in between the trap and the optical pumping field, I made the OP field go to zero to be able to see the differences more easily.

1.1.1 The Setup

To mimic the trap offline, we used a set of coils with almost the same inductance as the trap coils and they were in a stainless steel cylinder as shown below. On top and below the cylinder there were copper gaskets to imitate the real chamber. We then put a hall probe as close to the center of the coils as possible to be able to measure the magnetic fields.



Figure 1: Offline Coils

1.1.2 The Results

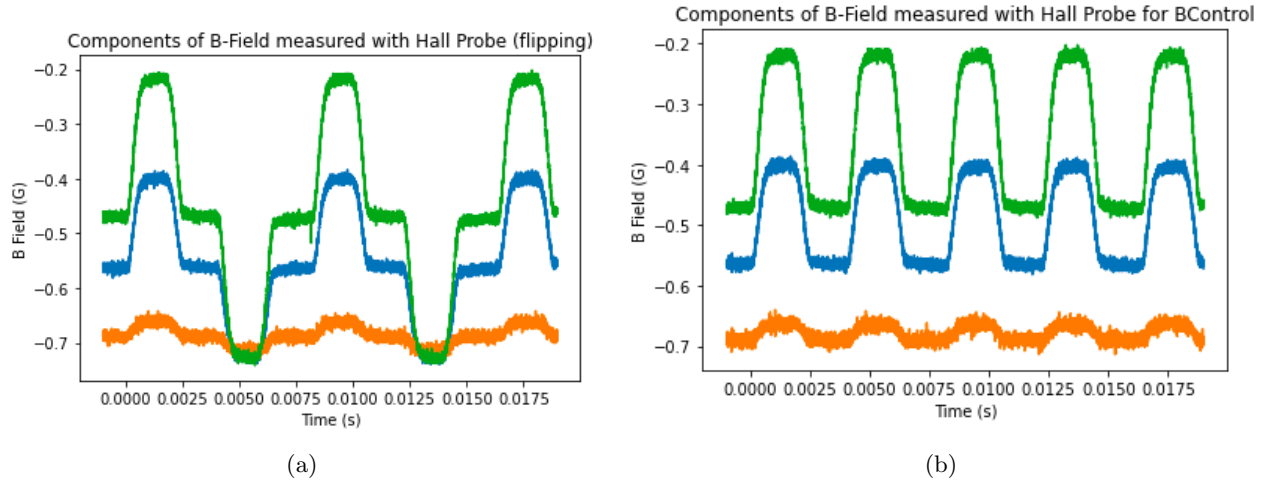


Figure 2: Magnetic Field measured with Hall Probe: Blue= B_x , Orange= B_y , Green= B_z

From figure 1, in the x and z components of the magnetic field, the field does not look to be completely flat during the time between trapping. Looking at the B_z component (along cylinder axis) in more detail, with an added smoothing function:

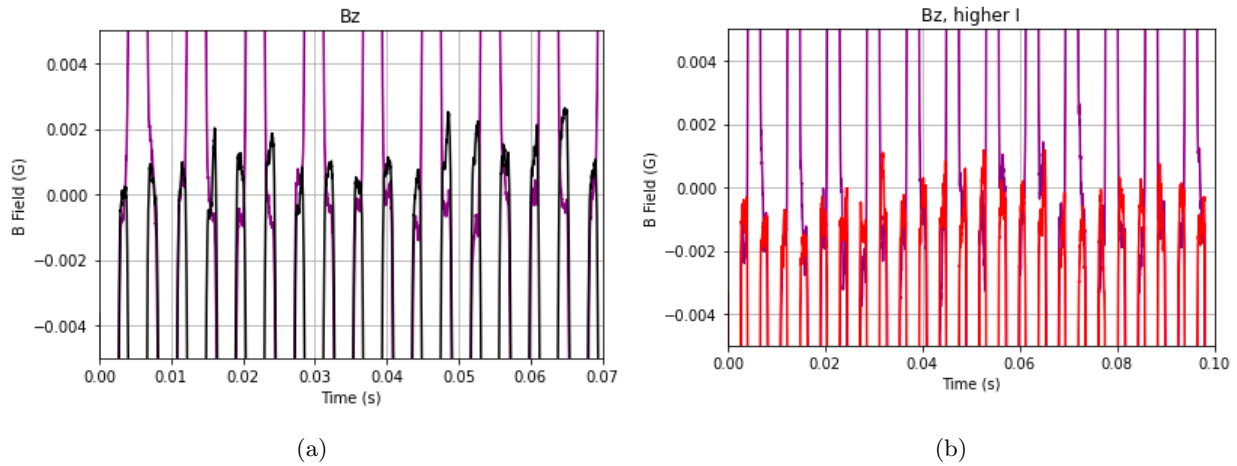


Figure 3: Z-Component of Magnetic Field with different currents: flipping=purple

In Fig 3, we only consider the B_z component of the magnetic field and we are looking how close to zero the times inbetween trapping cycles get over many cycles. In Fig 2.a, though both the flipping and non-flipping zero points fluctuate around zero, the flipping field seems to fluctuate slightly less. However, when we increase the current past the test current we had it at, the two waveforms are much more similar.

1.2 Trap EOM Control

For the position dependent portion of the MOT to work, the quadrupole field needs to match with the polarization of trap light in that direction (B -field is slightly negative, trap laser needs to be σ^+). Therefore,

the polarization of the lasers need to be switched every time we flip the direction of the magnetic field. All of the MOT light for the second trap goes through a single EOM, which is configured to rotate between vertical and horizontal polarization. The polarization is later converted into circularly polarized light through a quarter-waveplate later in its path. Two separate voltages need to be applied to get the different polarizations. We looked at the power EOM output through a polarizing beamsplitter and a colorPol, and manually adjusted the input voltage to the EOM to find the range. We then used the Quarto to continuously scan over that range, to find the maximum and minimum output power which corresponded to the two different polarization settings.

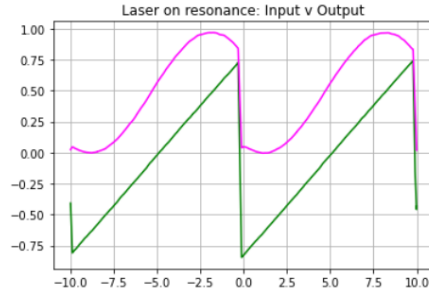


Figure 4: Trap EOM control

However due to the EOM's impedance, the voltage that we are trying to send to the trap is different than the voltage actually send, as seen by the figure below. Therefore, the values extracted from the above plot had to be scaled to what we were actually sending.

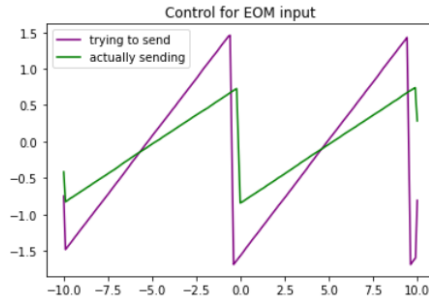


Figure 5: EOM Impedance Difference

The EOM switches sign 500us before the end of the optical pumping cycle. This way it will be switched before the magnetic field and it does not matter what its polarization is during the OP cycle since they use different lasers.

2 Fiber-coupled EOM at High Temperatures

2.1 Photorefraction Background

Lithium Niobate crystals (which two of our fiber-coupled EOMs are made out of) susceptible to the photorefractive effect.

With too much power going into the EOM, photogenerated electrons move from illuminated sections to dark sections of the EOM. This causes small local changes in the refractive index which can disrupt the EOMs ability to do frequency modulation. We are observing changes in transmission and suspect that this may be due to the photorefractive effect.

The photorefractive effect can be reduced by annealing the EOM. When the crystal is heated, the charge carriers can then move around and rearrange themselves, to have a more uniform distribution.

2.2 Heating the EOM

We were seeing reduced power through the EOM, it was stable and would degrade even further over time We added a strip heater to the bottom of the EOM and wrapped it a few layers of Teflon, then cut out a case of thick Teflon to cover it to ensure it was well thermally insulated. EOSpace recommends heating 40 degrees above room temperature to reduce the photorefractive effect. We were hoping to see the transmission through the EOM consistently improve as we raised the temperature.

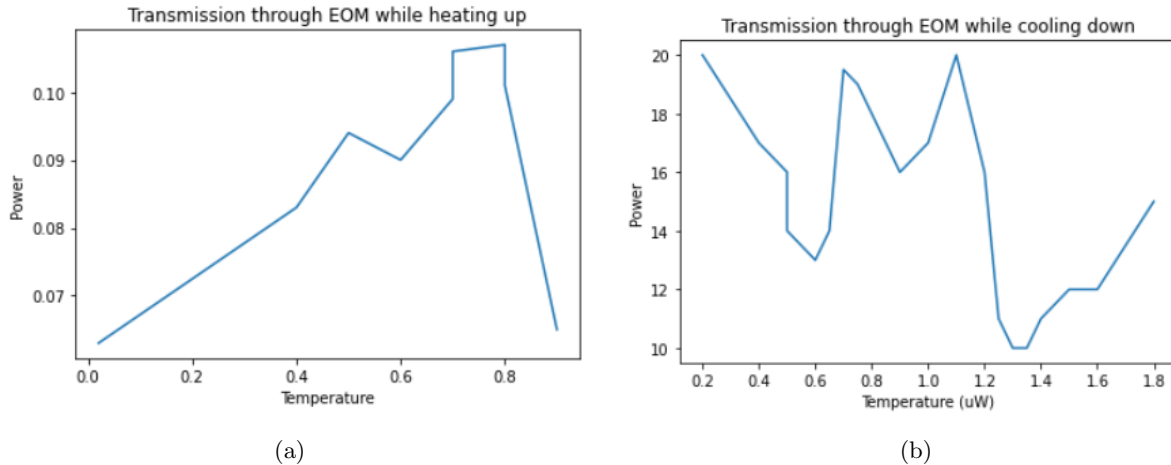


Figure 6: Transmission through EOM as the temperature changes

From the above figures, the temperature doesn't improve the transmission through the EOM - the polarization also drifted as the temperature increases, and had to be constantly adjusted to find the maximum - power drifted a little lower over long time periods

2.3 Possible Project

Newport also says that exposing the crystal to a UV light source can help to reduce the photo-refractive effect? This needs more research and an explanation as to why (I'm not seeing many other sources, in fact I'm finding sources saying that the photorefractive effect is actually increased). Did this work for Felix's report? Newport says there be internal components that may be damaged at elevated temperatures and to contact them first. Our fibers may also not transmit any UV light since its tuned for infrared.

3 Polarization

3.1 Extracting Data

During the beamtime, we tried to switch between sigma+, sigma-, and linear light in order every 30 minutes. We had trouble trapping the atoms and the EOM stopped transmitting most light on our last day. To analyze the data, I summed the runs all the 'good' data, and sorted by the polarization of the optical pumping light. I summed the root files, then extracted the ntuples and saved them as an ascii file. The root commands to do this are:

```
root filename.root (what file you want to open)
```

```

TTree *t = (TTree *)_file0 → Get("ntuple")
t
t → SetScanField(0)
.> newfilename.asc
t → Scan("TTTL_OP_Beam:QDC_OPon:TDC_ION_MCP_LE[0]:TDC_DL_X1_LE[0]:TDC_DL_X2_LE[0]:
TDC_DL_Z1_LE[0]:TDC_DL_Z2_LE[0]:TDC_PHOTO_DIODE_LE[0]:TDC_ELECTRON_MCP_LE[0]:
TTTL_Push_Beam");
.>

```

All my code for this can be found on trcomp, in the /hgallop/data folder. Below are the runs taken during the beamtime, classified into their respective optical pumping laser's polarization.

$$\begin{aligned} \sigma+ &= 4384, 4396, 4399, 4410, 4414, 4421 \\ \sigma- &= 4386, 4392, 4393, 4394, 4397, 4400, 4412 \\ \text{linear} &= 4387, 4395, 4398 \end{aligned}$$

3.2 Different Cuts

3.2.1 Looking at Position

We wanted to see how the position of the ions changed during the optical pumping time. To get these plots, add added TTTL-OPBeam cuts for a small sliver of time before the OP cycle (1000-1220) and just after (2400-2600).

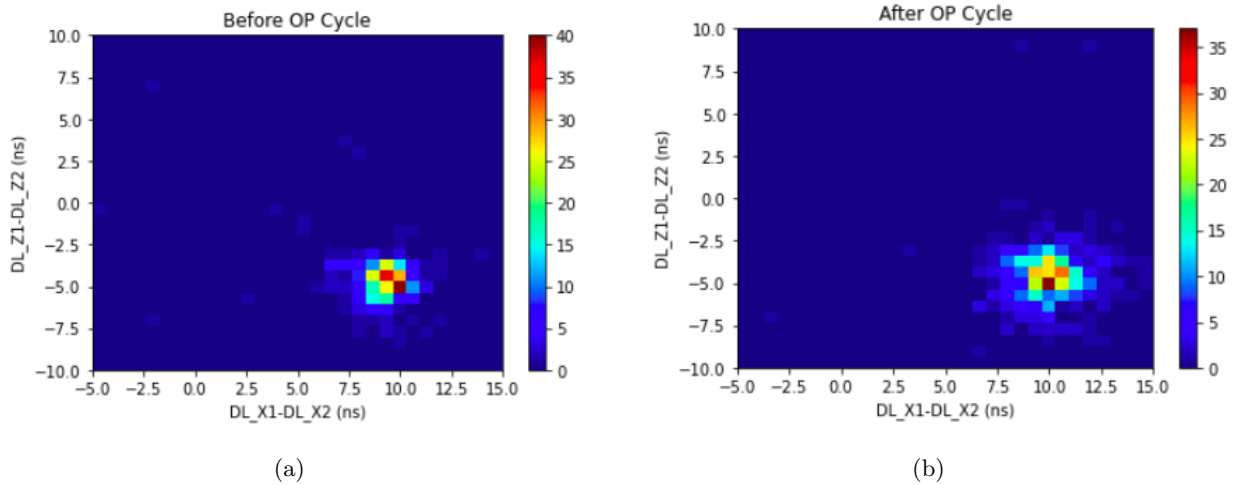


Figure 7: Ion Position of trapped atoms just before and after optical pumping cycle

The cloud of atoms expand between the two images. We expect to see this as the atoms aren't being actively trapped while they are being pumped. They also seem to have shifted slightly to the positive x-direction, and to the negative z-direction. This indicates the OP light is slightly moving the atoms. To get the position cut used later, the region is taken to be the tightest cut that still covers the shift we see in the atoms during the optical pumping time.

3.2.2 Push Beam

We included this cut to be thorough, however this ideally should not throw away any additional events as long as the QDC-OPon cut is applied. We only watch events when the push beam is not pushing atoms to the trap so we make a cut to only include events from 188 to 650 ms.

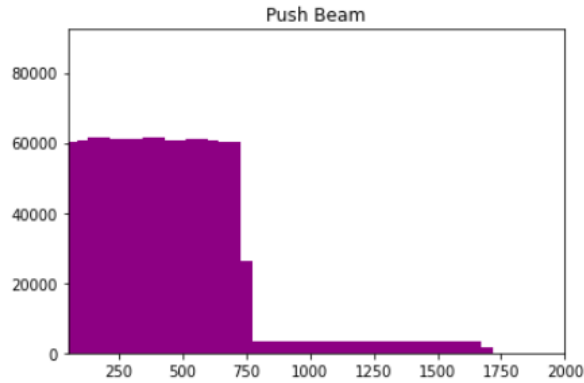


Figure 8

3.2.3 Photoion Events

To increase confidence that we are actually looking at photoion events, we perform an additional cut on the ion-photodiode timing. To get rid of all the background that is visible on the following plot, we restrict the events to those that occur between 1775-1825 ns.

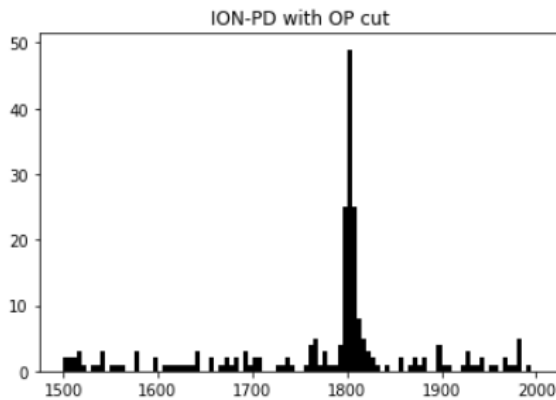


Figure 9: ION-PD [ns]

3.3 The odd Run 4389

This run was supposed to be a σ^+ , but at the end of the run when I went to go switch the polarization of the light, we found the program that sent the control to the TNLC had frozen. We restarted it but it still wasn't working and we switched to an older-model Meadowlark controller, which produced the same 2KHz square wave as measured on an oscilloscope. The resulting polarization from this still needs to be checked. However, we found this run to be an outlier compared to all other runs (linear and circularly polarized) and decided to exclude it from the analysis.

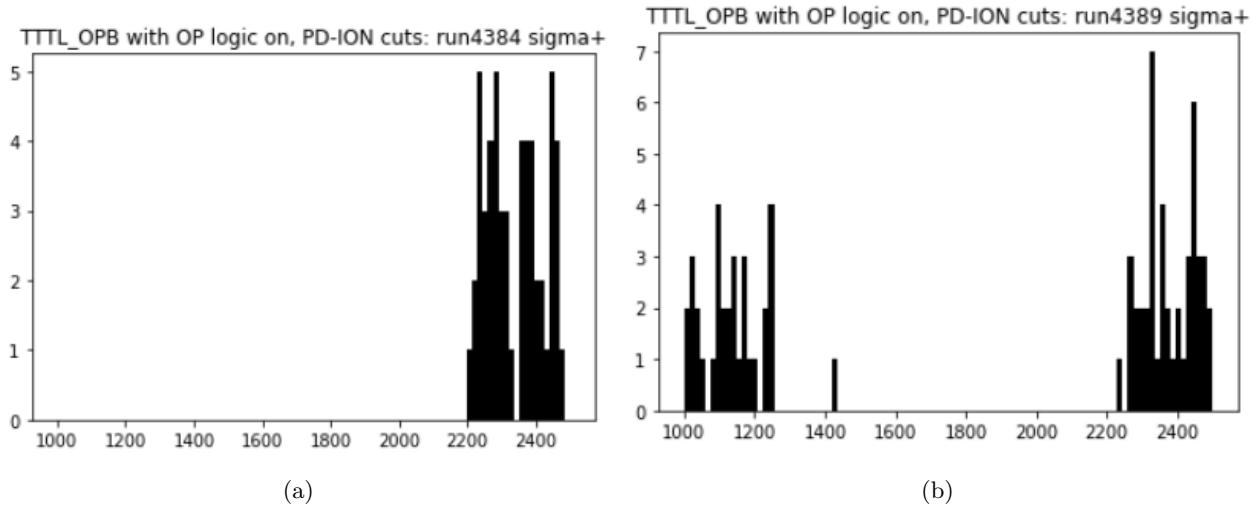


Figure 10: The difference in behaviour of Run 4389 vs another sigma+ run

As shown above, 4389 has many more events at the start of the optical pumping time (1100) compared to the rest of the circularly polarized runs. The only thing that changed (that we noticed) for this run is the optical pumping laser’s polarization so it is odd that the counts don’t match so drastically. We suspect the large number of counts towards the end of the cycle are the photoions from the trap light, and they are somehow passing through the OP on logic cuts. In the same manner, it possible the peak of photoions we see in run 4389 may be from MOT light as well.

We were not sure at which point the TNLC controller stopped working, so we were hoping we would be able to see differences in the photoions at the beginning of the run compared to the end of the run. This would allow us to use the start for polarization analysis. When the ntuples are extracted they are filed with a run number that corresponds to the order of events so I used this extra column to make the time cuts.

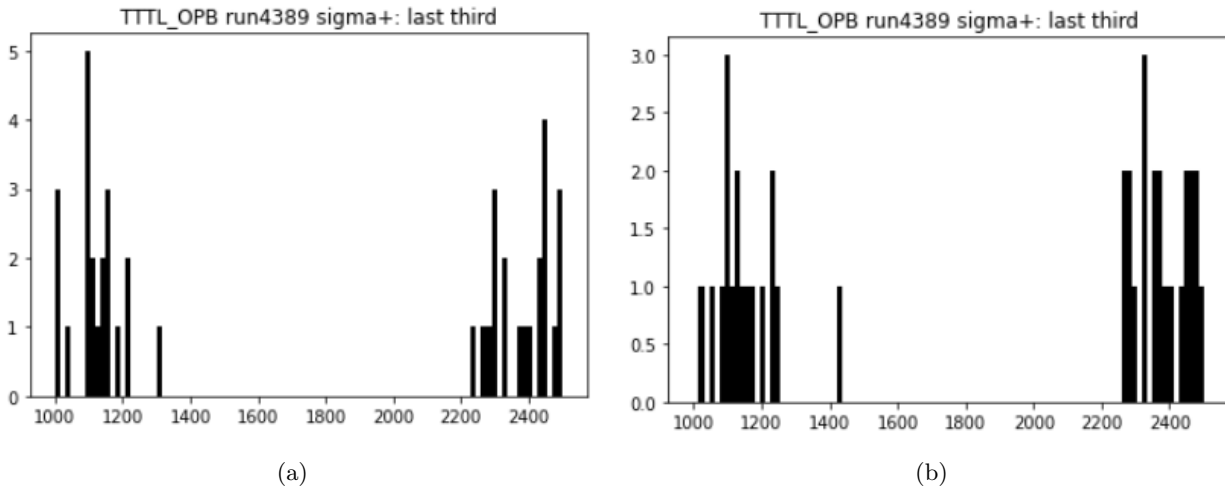


Figure 11: The difference in behaviour of Run 4389 vs another sigma+ run

However, we are still seeing multiple events around the 1200 mark in both plots. This implies that whatever was different about the run was consistent throughout the entire run, which makes the entire run unusable.

3.4 Best Estimate of Polarization

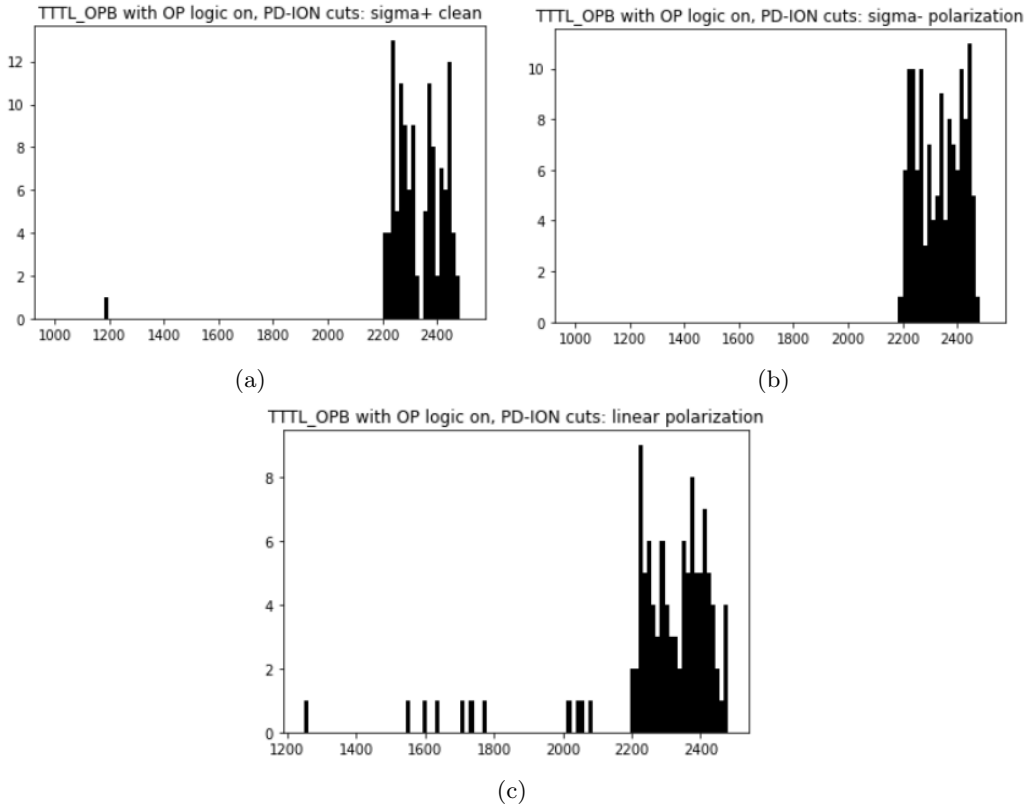


Figure 12: Photoion events for different polarizations of Optical Pumping light

We were hoping to see a peak of early on in the optical pumping cycle for both the circular polarization sums. However, we only see one event around 1200, which isn't quite enough to use to make an estimate for polarization the same way I did in my previous report for 41K. However, there are clearly more events during the optical pumping region during the linear polarization which means we can estimate the expected rate during the optical pumping time. Compared to 41K, the rate should be 2-3 orders smaller as the number of atoms trapped is 10^3 instead of 10^5 or 10^6 . The time it takes to optically pump is also different for 41K to 47K since it scales with the number of states squared, so in 47K it is $\frac{4}{8} * 2 = \text{frac}14$. Therefore we would expect to see only a couple events in the optical pumping peak, instead of the larger number we saw with 41K.

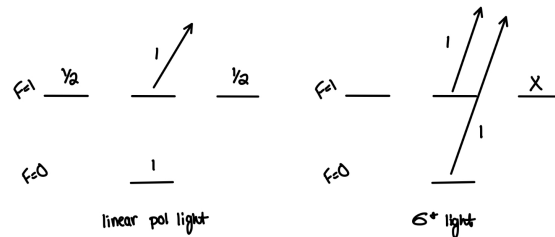


Figure 13: Transition Strengths for the different polarizations of light

The pumping scheme is different depending on what type of light is used. Since what we call 'linear light' is actually sigma+ and sigma- being applied in opposite direction, we can estimate the 'linear polarization' as being an even superposition of right and left circularly polarized light and the transition strengths are as shown

in the sketch above. This does not consider the effects the possible standing wave from the two optical pumping lasers.

We can make an estimation for the number of unpolarized atoms during optical pumping based of this based off the fact that the counts we see during the optical pumping time are from the transition strength multiplied by the population in these states.

T = average transition strength, R = count rate

$$\frac{R_{linear}}{R_{circular}} = \frac{T_{lin} * Pop_{lin}}{T_{circ} * Pop_{circ}}$$

We now define $\epsilon = 1 - x$, the number of atoms not in the fully stretched state during optical pumping with circularly polarized light. If we assume that all the states are uniformly populated throughout the optical pumping time for linear light, and that the $m_F = -1$ state doesn't contribute much to the excited state for circularly polarized light, we get:

$$\frac{R_{linear}}{R_{circular}} = \frac{3}{4 * \epsilon}$$

From looking at the plots, we can easily count the events during the optical pumping time, and when I summed all the runtimes for each polarization, circularly polarized light ran for 3.63 times longer than linear light.

$$\begin{aligned} \epsilon &= \frac{3}{4} \frac{N_{circ}}{N_{lin} * 3.63} \\ \epsilon &= \frac{3}{4} \frac{1}{11 * 3.63} \\ \epsilon &= 0.02 \end{aligned}$$

If we only consider the statistical error from the counts, and the error on N_{circ} is ± 1 , this gives an uncertainty of 104 percent on ϵ

$$\Delta\epsilon = \epsilon * \sqrt{\left(\frac{\sqrt{11}}{11}\right)^2 + \left(\frac{1}{1}\right)^2}$$

$$\Delta\epsilon = \pm 0.02$$

Therefore we can say $2\% \pm 2\%$ of the atoms are not in the fully stretched state during optical pumping. This could indicate a high polarization, however we need decay observables like beta-asymmetry to confirm.

3.4.1 Differences on how normalize the count rate

In the previous section, we were normalizing the counts by the amount of time we were collecting data over. However, the decay rates and photoion events are not equal throughout all the runs as there were various issues with our trap during the beamtime. We could also normalize the counts based on the number of total-photoion events recorded (not just during OP time) or the number of decay events.

Normalization	Sigma+	Sigma -	All Circular
Run time	0.04 ± 0.04	0.04 ± 0.04	0.02 ± 0.02
Num of events	0.05 ± 0.05	0.04 ± 0.05	0.02 ± 0.02
Num of decays	0.06 ± 0.06	0.04 ± 0.04	0.02 ± 0.02

Table 2: Different ways of calculating ϵ

3.5 Estimation of Background

The ion MCP detects that recoil ions for the 47K beta decay, and if these events happen to coincide accidentally with the UV laser pulses, they create a background signal. So to estimate the background, we looked at the timing of the ION_MCP and the photodiode difference. As explained in **input section number here**, we usually use this spectrum to provide an additional cut on the TTTL_OPBeam spectrum.

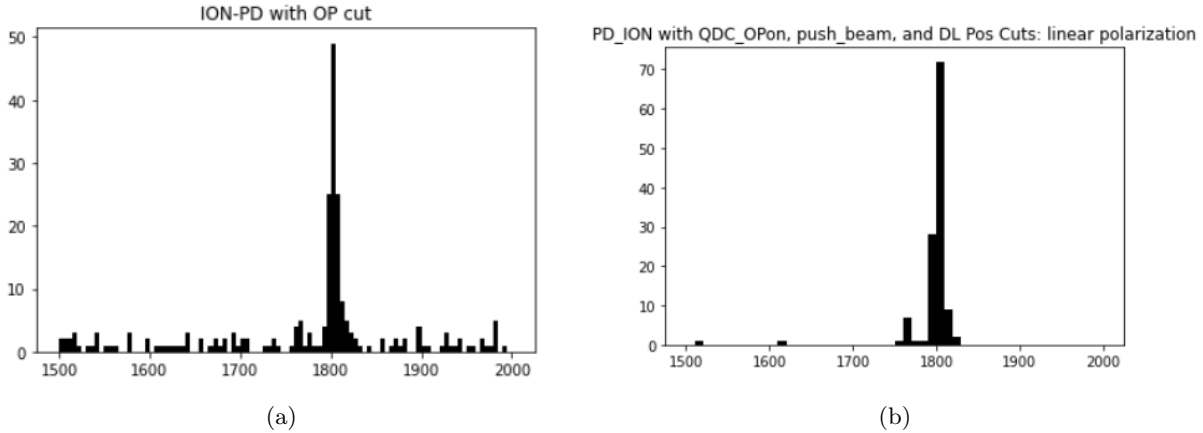


Figure 14: ION-Photodiode timing with and without the position cut for linear light

With the position cut applied, we clearly get rid of most of the background, although a little sneaks through. Since 4 counts of background occur over 450ns, and the region we cut over to analyze is only 50ns we expect to see than than one count (0.44 ± 0.22) in the peak.

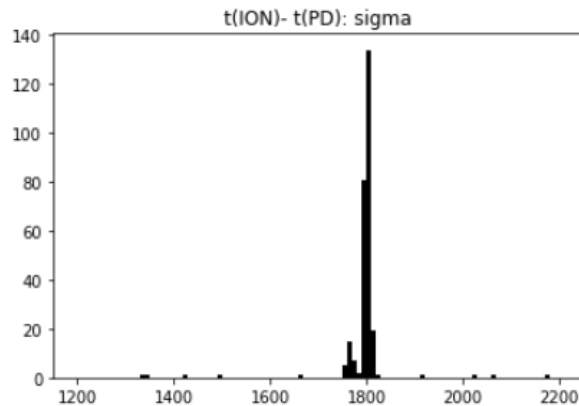


Figure 15: ION-Photodiode timing with and without the position cut for circular light

Checking with all the circular light as well, we find 9 counts over 900ns, giving an expected background of 0.50 ± 0.17 counts over the 50ns region where we cut. These two values agree with each other within the uncertainty bounds, and we would expect the same background no matter what they polarization of optical pumping light is.

3.5.1 Why don't we see a peak at the start of the optical pumping time

47K is a $I=1/2$ structure, unlike 41K which is $I=3/2$. Since there are less states in 47K compared to 41K, the speed to pump is quicker, at $\frac{1}{4}$. 47K also has 2-3 orders less of trapped atoms so we expect to see less events in general. Further more the optical pumping power was weaker (by half) since we switched from double EOMs to just one and lost power to a fiber splitter. It is possible that the atoms are pumped very quickly and more weakly and we just don't see enough events at the detectors. Or we are simply not pumping any others, but the difference between linearly polarized light and circularly polarized light shows that the optical pumping lasers are interacting with the atoms in some way.

4 Detectors

4.0.1 Summary of Scintillation Crystals

We use scintillation detectors to monitor the gamma rays emitted from the beta decay. The scintillation detectors essentially convert the high energy gamma rays into multiple lower energy photons (GAGG = 50,000 optical photons / MeV, NaI = 40,000 photons / MeV, BGO = 9,000 photons / MeV [2]) that can be detected by our Silicon Photomultipliers (SiPMs), which are then able to convert the light signal into an electrical signal that we can analyze.

4.1 Sodium Iodide dope with Thallium (NaI:Tl) Scintillation Crystal

We are currently using GAGG crystals as our scintillation detector, however Brian noticed that using a NaI detector may provide us with better photodetection efficiency since the wavelengths the NaI crystal emits better matches with the optimal performances of the silicon photo-multipliers we are using. We happened to have one in the lab, so we decided to test it out to see if it was a good idea to include it in the upcoming beamtime run.

4.1.1 Assembly of NaI

The NaI crystal was slightly larger than 2inch so we mounted it in a 3inch optics tube with a layer of foam around it to prevent it from moving. We also wrapped it in a layer of thin teflon to reflect the light so the scintillation light doesn't escape and is detected as much as possible.



Figure 16

We then clamped it in place using an O-ring and a 3 to 2 inch optics tube adapter. We cut out a piece of thick teflon with a square cut out in the center for the SiPMs to fit, the square was cut from the outline of the SiPM board exactly. Inside the cut out square we put a piece of optical (silicon based) gel that has a similar index of refraction as the NaI to smooth the transition to the SiPM.



Figure 17

We used Tine's board (see his report) to attach to the crystal. His board has a 2x2 set up of J-type SiPMs.

4.1.2 Calibration of NaI

We bias the detectors by applying a voltage across the SiPMs. We increase the magnitude until we reach the breakdown voltage, where the current readout increases suddenly. Each of the SiPM arrays need to be biased above the breakdown voltage in order to detect individual photons.

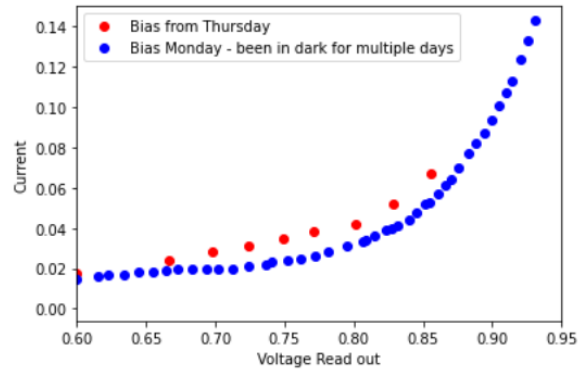


Figure 18

From this plot, we can see that the voltage breakdown starts around $0.8 \times 32V = 25.6V$, so we need to be at a larger value than this. To calibrate the detector, we put it next to a Co60 sources, which also has 137Cs contaminate in it.

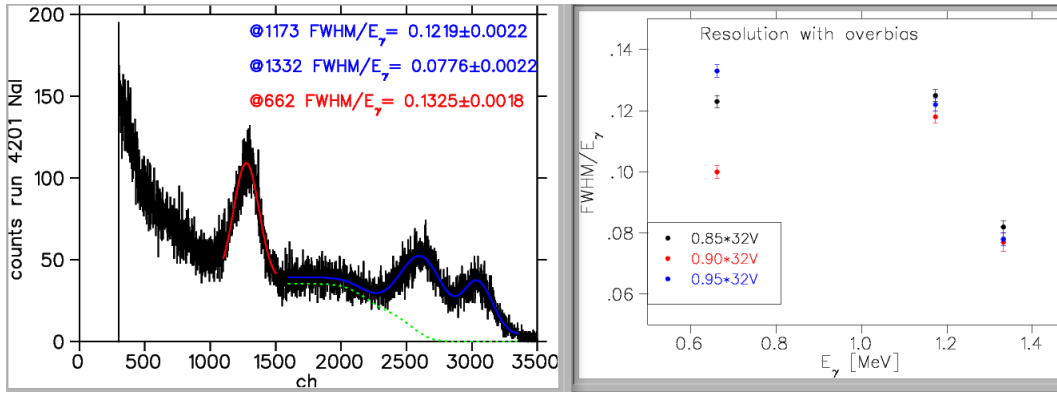


Figure 19: NaI Spectrum next to Co60 + 137Cs. Plot from elog Nuclear tests 89, by John Behr.

We ran at multiple different overbiases, and very hoping to see an indication of improvement in energy resolution as the voltage increases. However, as seen in the above figure, there is no strong indication of this. Furthermore, the photo efficiency decreases at higher energies and we decided that the photo efficiency was too low at the gamma ray energies we would actually use in our experiment. Therefore, we decided not to include the NaI crystal in our beamtime setup.

I determined the FWHM of the peaks for 137Cs with NaI, then calibrated the sigma using the Compton edge to gamma peak distance. I then used this sigma to attempt to estimate the resolution at the 586.0 and 564.8 keV energy peaks. I also adjusted them according to their relative strengths and summed them to best estimate what we would actually see. From the figure, we can tell that these two peaks are not distinguishable from each other using the NaI scintillation crystal.

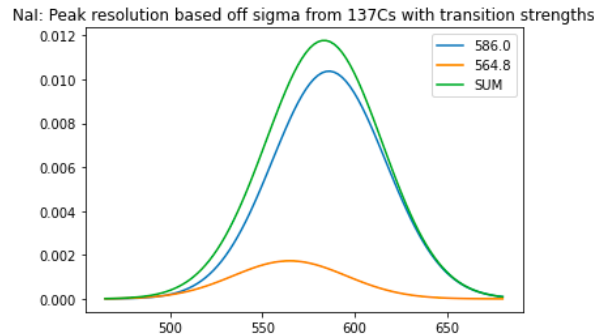


Figure 20

4.2 Bismuth Germanate (BGO) Crystal

Compared to NaI(Tl), a BGO crystal is denser and is denser material and is therefore supposed to have a better photo efficiency, however this also leads to a lower energy resolution. Since the NaI scintillation crystal wasn't going to work, we decided to compare a BGO crystal.

The assembly of the BGO scintillation crystal was very similar to the NaI, however it was smaller and fit inside at 2inch optics tube and we added an additional layer of dielectric film to help it stay light tight. We switched over Tine's board to couple with and used the same silicon gel as well.

4.2.1 Calibration of BGO

When biasing the BGO, we found that the current increase was a larger value than with the NaI, however it was still linear for the most part so we continued using it. It also was a little unstable around and above the breakdown voltage, the current value would decrease a little bit after it was adjusted. For reading the energy spectrum's, we set the bias voltage to $0.900 \times 32V$ since the breakdown voltage is around $0.800 \times 32V$. We ran at this voltage for NaI as well.

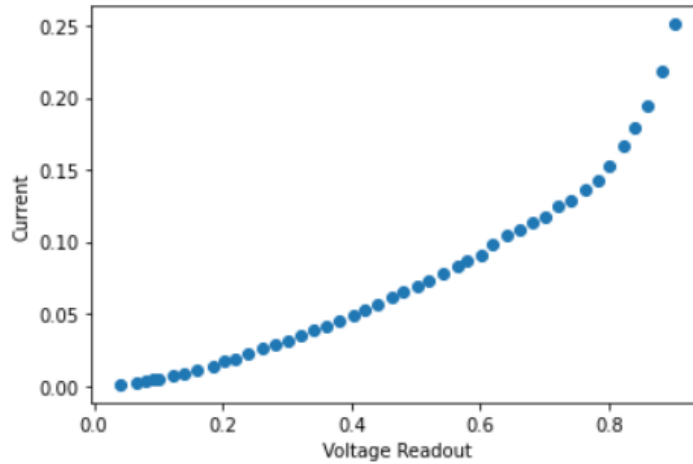


Figure 21: BGO Bias Voltage

We took a run with the same Co60 source that has 137Cs contamination that we used for calibrating Cs137. The large peak at channel 650 is likely from a mix of Co60's energy peaks at 1172 keV and 1333 keV. The energy resolution is clearly worse than the NaI as we aren't able to resolve them as multiple peaks like we were in NaI.

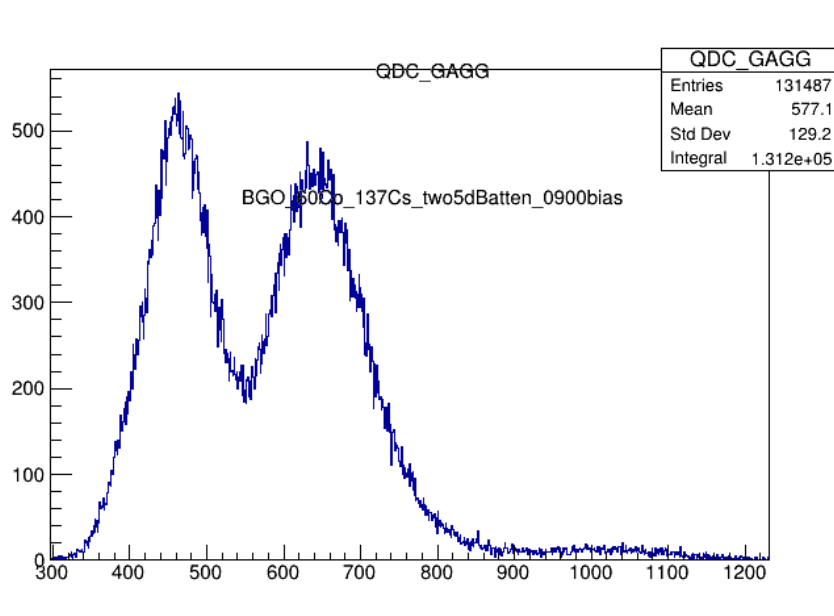


Figure 22: BGO Energy Spectrum next to Co60 + 137Cs.

However, to implement this we would have had to move the GAGGs and messed with the UV alignment

which would take a lot of time with no guarantee that it would work, so we decided not to use the BGO before the beamtime.

5 Pumping Schemes for 40K vs 47K

John's elog under 'resources' has the D1 transitions for both isotopes.

5.1 Locking 47K

47K : $J = \frac{1}{2}$ $I = \frac{1}{2}$ $F=1$

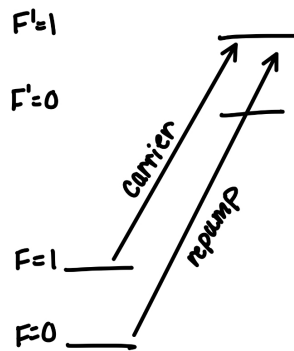


Figure 23: 47K Structure

Put the carrier on 47K's $F=1 \rightarrow F'=1$ transition: 105.43 MHz / Put the repump on 47K's $F=0 \rightarrow F'=1$ transition: 3525.63MHz

Lock to 39K's crossover ($F=2 \rightarrow 1'$)($F=2 \rightarrow 2'$) peak: -180.MHz

$$\nu_{trap} = \nu_{lock} - 2 * \nu_{AOM.12} + \nu_{AOM.SAS}$$

Since AOM12 is always at 101.7 MHz, we can set AOMSAS to -76.86 MHz, which is technically outside of the bound of the AOM (85MHz - 130 MHz) but we ran here and it was fine.

5.2 Locking 40K

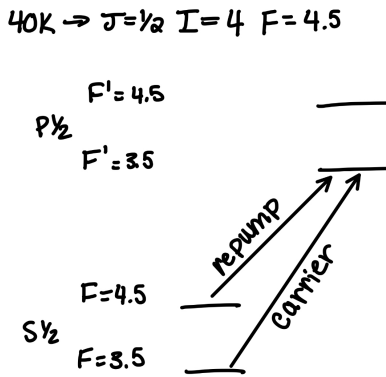


Figure 24: 40K Structure

Put the carrier on 40K's $F=3.5 \rightarrow F'=3.5$ transition: -502.38 MHz / Put the repump on 40K's $F=4.5 \rightarrow F'=3.5$ transition: 783.41 MHz

Lock to 39K's crossover ($F=2 \rightarrow 1'$)($F=2 \rightarrow 2'$) peak: -180.MHz. Using the same process as the previous section, we put AOMSAS to 95.3 MHz to get to the carrier frequency.

5.3 Adjusting EOM circuit between 40K and 47K

For 47K, the repump frequency is 3525.6MHz, which is 3420.19 MHz away from the carrier frequency. So we need side bands at 3420.19 MHz, which is much larger than the sidebands we had for 40K (which has sidebands at 1285 MHz), so almost all of our circuit components have to be switched when we switch what we are pumping.

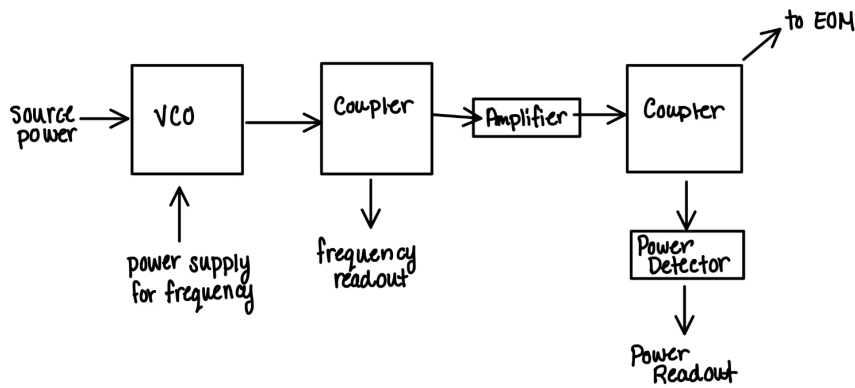


Figure 25: EOM RF Circuit

	47K	40K
VCO	PE1V31027	ZX95-1570-S+
Couplers	ZADC-10-63-S+	ZABDC20-182H-S+
Amplifier	ZADC-4016E-S+	ZX60-P103LN+
Powerdetector	ZX47-40LN-S+	ZX47-40LN-S+

Table 3: Electronic Components Used for each isotope

Side note this is the set up just for adding sidebands using the EOM. At the end of the semester, John and I tried using direct RF injection which required a lot more power so we switched out the amplifier and the VCO, and we still only saw very small (2%) sidebands.

6 Camera/ Octave Scripts

The firefly camera has been placed at the viewport of the MOT and has previously been used to monitor the atoms fluorescence to see if we actually have trapped atoms. However, there are much 47K atoms and the trap is more difficult to visualize so we need to sum multiple images. To do this, we edited codes written by a previous co-op student, Andrew Kovachik.

6.1 Accessing and executing the scripts

All of the camera scripts are on **trinat-black**, including Andrew Kovachik's original scripts. First ssh to this computer:

```
ssh -Y trinat@trinat-usb-eth5
```

You need two terminal windows open, one to run the summing script and one to run the camera trigger script.

We need to subtract background off of the images we collect, so before running the summing function, you have to turn the trap off and collect background images. These scripts are kept in a different directory than the summing function.

First in the trigger terminal window:

```
flycapture2019/bin/$ AsyncTriggerJB47K
```

In the summing terminal window:

```
cd /photoAnalyses
```

```
octave BackgroundSumming.m
```

This is going to collect about 20 images and sum them, then save them as a file labelled 'Background.bmp'. This new file needs to be moved to flycapture2019/bin where all the other images are going to be kept. In the flycapture/bin directory, there are going to be old images from the previous run, these need to be moved to another place so they don't contaminate the new set of data.

To actually run the summing script once you have a background image and have emptied all other .bmp files from flycapture2019/bin.

In trigger terminal window:

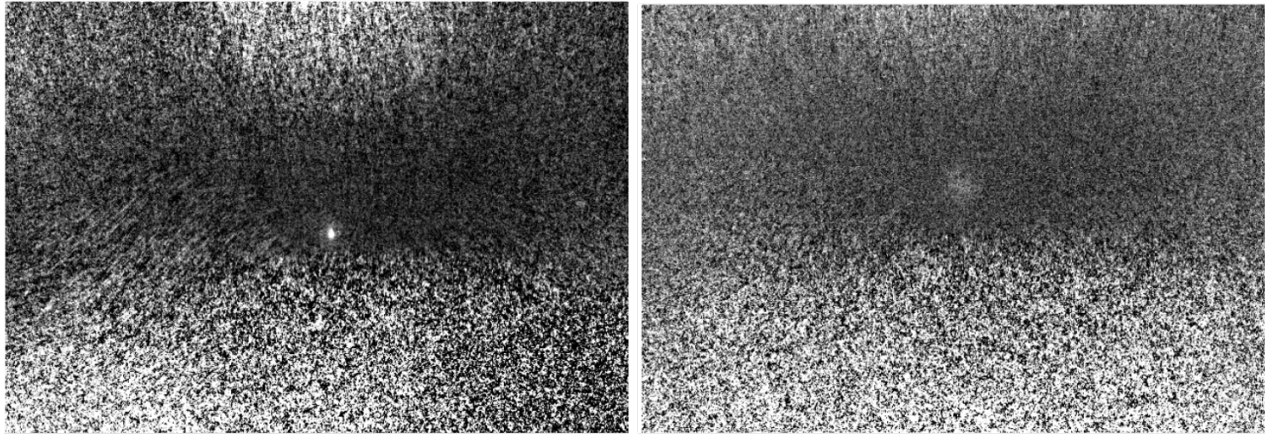
```
/flycapture2019/bin/AsyncTriggerJB47K
```

In summing terminal window:

```
photoanalyses/$ octave SumIn.LightCurve.m
```

This is going to sum any new pictures in the flycapture/2019 directory, subtract 'Background.bmp' and project the final image to the screen.

6.2 47K Run



(a) DC MOT

(b) AC MOT

Figure 26: Images of the 47K trap summed with SumIn.LightCurve.m

Figure 26 shows two of the images taken during of 47K August beamtime, and they both show evidence of a trap. The DC trap is more condensed and closely confined, whereas the AC MOT is more spread out which is to be expected. However, both of the traps look to be off center which implies that the trapping lasers are unbalanced and potentially need to be better aligned.

References

- [1] Melissa Anholm, Ph.D. Thesis, U Manitoba, Dec 2022
- [2] BERND J. PICHLER, SIBYLLE I. ZIEGLER, Emission Tomography, 2004